CrystEngComm

PAPER

View Article Online
View Journal | View Issue

Cite this: *CrystEngComm*, 2024, **26**, 3634

The role of cavitation and gas bubbles in the non-photochemical laser-induced nucleation of sodium acetate†

Eleanor R. Barber,[a] Martin R. Ward [b] and Andrew J. Alexander *[a]

An experimental study of the effects of the sodium salt of poly(methacrylic acid) (Na-PMAA) on non-photochemical laser-induced nucleation (NPLIN) of sodium acetate crystals is presented. Seeding of supersaturated aqueous solutions with anhydrous (AH) seeds always produced trihydrate (TH) crystals, with or without polymer additive. Using NPLIN, with no Na-PMAA and at low Na-PMAA concentrations (0.25% w/w) AH sodium acetate was produced, firstly as plate-like form IV, but subsequently growing needles, likely to be form I. At high Na-PMAA concentrations (0.73% w/w) we observe formation mostly of stable bubbles. In all samples at low laser peak power densities (<26 MW cm^{-2}) we show for the first time using NPLIN that both crystals and bubbles can be nucleated with a single laser pulse. Measurements of the dependence of bubble or crystal count on laser pulse power indicate a common mechanistic origin for nucleation, which is cavitation due to laser heating of impurity nanoparticles. The bubbles observed are attributed to laser heating of the nanoparticles to high temperatures, resulting in gas formed by thermochemical reactions or gas that was previously dissolved in the solution. Our results provide new insight into the particle-heating mechanism for NPLIN, but whether stable bubbles play a defining role in the nucleation of crystals remains to be resolved.

Received 14th May 2024,
Accepted 11th June 2024

DOI: 10.1039/d4ce00487f

rsc.li/crystengcomm

1. Introduction

Laser-induced nucleation (LIN) is a method for rapidly stimulating growth of crystals, often producing unexpected crystal morphologies and habits. LIN can be classed broadly into optical-trapping and pulsed-laser methods. Optical trapping-induced crystallization (OTIC) uses tightly focused laser light, usually continuous-wave.[1] Using this method, for example, Wu *et al.* showed control over hydrate formation in the crystallization of L-phenylalanine from aqueous solutions.[2] The use of laser pulses to induce nucleation at wavelengths where absorption by the system is minimal is commonly referred to as non-photochemical laser-induced nucleation (NPLIN).[3] Li *et al.*, for example, demonstrated that NPLIN can produce different polymorphs of sulfathiazole from supersaturated solutions when using different polarizations of light.[4] Higher laser-pulse powers, *e.g.*, through focusing the beam or shortening the pulse length, can also cause LIN through photochemical and photomechanical processes such as plasma production and cavitation.[5–8]

Details of the mechanisms for all classes of LIN are still under scrutiny. As discussed by Alexander and Camp, heating of solid impurity nanoparticles by the laser light now seems to be the most likely mechanism for NPLIN.[9] The heating of nanoparticles to temperatures above the critical temperature (*e.g.*, 647 K for water) results in spontaneous vaporization of fluid surrounding the particle, creating a cavity that is expected to rapidly expand and subsequently collapse, *i.e.*, thermocavitation.[10,11] The strongest evidence for this mechanism comes from the observation that nanofiltration of solutions reduces or switches-off NPLIN; while intentionally doping filtered solutions with nanoparticles can reactivate NPLIN.[12–14] The mechanistic details of how thermocavitation leads to nucleation of solid crystals, however, is not clear. Comparison against other induction methods that are thought to involve cavitation, such as sonocrystallization and mechanical shock, suggest that the thermocavitation events in NPLIN are more energetic, or hotter.[15] In the case of NPLIN of glycine from aqueous solutions, switching in preference from the α to the γ polymorph of glycine with increasing supersaturation was observed to be sharper compared to sonocrystallization or mechanical shock.[15] For NPLIN of NaBr, it was observed that NPLIN favoured nucleation of the

[a] *School of Chemistry, University of Edinburgh, Edinburgh, EH9 3JJ, UK. E-mail: andrew.alexander@ed.ac.uk*
[b] *CMAC, University of Strathclyde, Technology and Innovation Centre, 99 George Street, Glasgow, G1 1RD, UK*

† Electronic supplementary information (ESI) available. See DOI: https://doi.org/10.1039/d4ce00487f

anhydrous salt, whereas spontaneous nucleation favoured the dihydrate.[16]

Sodium acetate trihydrate ($CH_3COONa{\cdot}3H_2O$) is a well-known example of a phase-change material (PCM): a substance with a high latent heat associated with a liquid–solid or solid–solid phase transition. PCMs have promising applications in thermal-energy storage, as they can release or absorb heat on freezing and melting.[17,18] A small-scale example of this is the use of sodium acetate trihydrate in reusable handwarmers. These are pouches of supersaturated aqueous sodium acetate, prepared by heating in boiling water and cooling to room temperature. Flexing a metal disk contained within the pouch ejects seed crystals trapped within grooves and initiates crystal growth, through which the latent heat is released (see ESI,† Fig. S1).[19] The pouch can be reheated and reused multiple times.

On a larger scale, sodium acetate trihydrate (TH) is a prime candidate for the heating of domestic water, due to its convenient melting point and large latent heat of fusion (226–289 kJ kg^{-1}), as well as its low cost, low toxicity, lack of corrosiveness and non-flammability.[17,20–25] However, a major barrier is the formation of the anhydrous (AH) salt, which is difficult to redissolve and can form in significant quantities over multiple nucleation and heating cycles.[26] This leads to a reduced latent heat and a less well-defined melting point. To overcome this problem, investigations were carried out to identify polymer additives that can inhibit the nucleation of anhydrous (AH) sodium acetate.[26,27] Oliver *et al.* discovered that the sodium salt of poly(methacrylic acid) (Na-PMAA) was an effective inhibitor; a minimum concentration of 0.67% w/w polymer was required to suppress AH sodium acetate in a solution containing 41.5% water and 57.8% sodium acetate (C = 17.0 mol kg^{-1}).[26,27] The mechanism of inhibition is unknown, but it has been proposed that carboxylate groups on the polymer chain bind to sodium ions associated with either solute clusters or specific surfaces of crystallites, preventing their further growth.[26]

In NPLIN experiments carried out by Liu *et al.* with pulsed near-infrared laser light,[28] it was shown that AH sodium acetate was nucleated exclusively. The addition of the polymer nucleation inhibitor Na-PMAA to the samples produced some interesting effects. At lower polymer concentrations (0.06–0.10% w/w) crystal growth was slowed; at higher concentrations (0.5–1.0% w/w) crystal nucleation was completely inhibited, but small bubbles were observed.[28] In contrast to a cavity, a bubble has sufficient internal pressure to persist for some time; a cavity will collapse due to its lower internal pressure, with a lifetime on the order of tens to hundreds of microseconds.[6,29,30]

In the present work we have explored NPLIN in sodium acetate solutions to understand the underlying mechanisms. The effect of laser pulse-power density on the number of crystals or bubbles was investigated. We show for the first time using NPLIN that both crystals and bubbles can be nucleated with a single laser pulse. We demonstrate that the NPLIN of crystals and bubbles share a common mechanism, which is cavitation due to particle heating. We propose that the persistent bubbles observed result from thermochemical reactions that produce gas, or nucleation of dissolved gas in the fluid surrounding the nanoparticle. Whether these stable bubbles are intermediates in the nucleation of crystals by NPLIN, however, remains to be resolved.

2. Experimental methods

Supersaturated aqueous solutions of sodium acetate (Acros Organics, anhydrous, 99+%) were prepared by dissolving the anhydrous solid in ultrapure water (18 MΩ cm). All samples had a sodium acetate concentration C (molality) of 16.7 mol kg^{-1}. Additionally, Na-PMAA was included in the solutions in varying quantities (Sigma Aldrich, average $M_n \sim 5400$, average $M_w \sim 9500$ by gel-permeation chromatography, received as 30% w/w solution in H_2O). Three groups of samples were prepared, categorized by Na-PMAA concentration, which we refer to by the weight percentage of polymer in the final solution: no Na-PMAA (0% w/w), low Na-PMAA (0.25% w/w), and high Na-PMAA (0.73% w/w). Dissolution took up to two days at temperatures of 60–75 °C. Solutions were transferred into glass vials without filtration. Each vial was filled with approximately 1.5 mL of solution. Samples were cooled in air for 3–4 hours to 25 °C, at which temperature the saturation concentrations (C_{sat}) are 6.14 mol kg^{-1} for sodium acetate TH and 15.2 mol kg^{-1} for AH sodium acetate.[20] The resulting supersaturations ($S = C/C_{sat}$) were 2.72 with respect to the hydrate and 1.10 with respect to the anhydrous salt; the location on the concentration–temperature phase diagram is shown in Fig. 1.

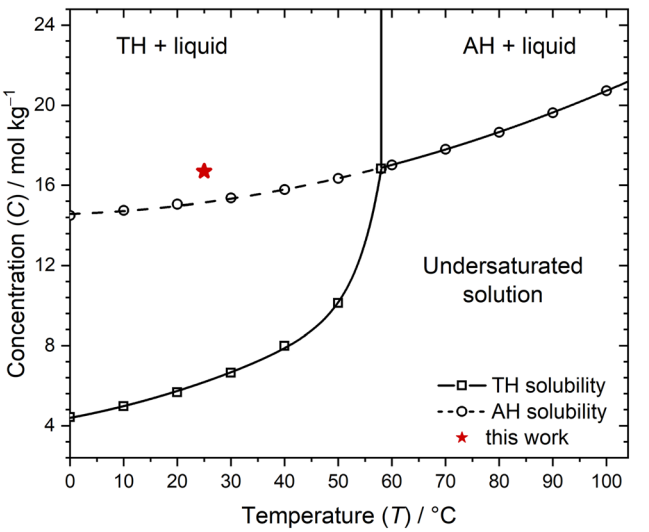

Fig. 1 Concentration–temperature phase diagram based on solubility data for sodium acetate in water (open circles).[20] The thermodynamically stable solid forms are indicated on the plot (AH = anhydrous; TH = trihydrate). The curves represent quadratic (AH) and exponential (TH) model fits to the solubility data, respectively. The experimental conditions used in the present work are indicated by a solid star.

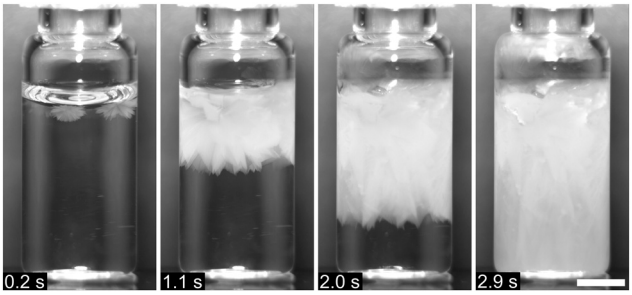

Fig. 2 Seeding of AH sodium acetate crystals into a supersaturated aqueous sodium acetate solution (C = 16.7 mol kg^{-1}, S = 2.72) containing high Na-PMAA polymer additive (0.73% w/w) *via* a needle through a septum in the lid. From left to right, images show the sample 0.2, 1.1, 2.0 and 2.9 s after seeding. Complete crystallization took place within 2.9 s, yielding TH crystals. Seeding into an open container and into a solution containing no Na-PMAA produced identical results. The scale bar represents 5 mm.

Sample vials were exposed to a single pulse (duration 5.0 ns) of laser light from a Q-switched Nd^{3+}:YAG laser (Continuum Surelite II-10, at 532 nm). The beam diameter was 4.8 mm and the incident pulse energies were 5.0–65 mJ, corresponding to pulse energy densities of 28–360 mJ cm^{-2} with peak power densities of 5.2–68 MW cm^{-2} (see ESI,† Table S1 and Fig. S2).[31] Imaging of the samples during and after NPLIN was carried out using a digital camera. Seeding of samples was also tested, either by removing the cap from a sample vial and adding a small crystal of AH sodium acetate, or through the septum of a sealed vial, using a needle to pierce the cap and drop a crystal into the solution. After samples had been nucleated, they were regenerated by reheating to dissolve.

3. Results and discussion

3.1 Seeding

The effect of seeding small crystals of AH sodium acetate into a supersaturated solution containing polymer additive (high Na-PMAA, 0.73% w/w) is shown in Fig. 2. Crystals of TH began to grow outwards immediately on contact of the crystallites with the solution, and rapidly spread throughout the vial. Within 3 seconds, complete crystallization had occurred, and the vial was warm to the touch. Identical results were observed whether the seeding was carried out into an open vial or through the septum of a sealed cap; or in solutions containing no Na-PMAA or high Na-PMAA. Submerging the tip of a needle into the solution had the same effect as seeding with a crystal. These observations are similar to those of Liu, who did not use polymer additive, and Oliver *et al.*, who used TH rather than AH to seed solutions containing polymer additive.[26–28]

Sodium acetate TH is the most thermodynamically stable form at room temperature.[20] Given that the solutions had a much higher supersaturation with respect to the TH than AH form (solid star, Fig. 1), the nucleation of TH *via* seeding is perhaps not surprising; this is the nucleation that occurs in reusable handwarmers. It is interesting to note, however, that seeding with AH crystals resulted in the nucleation of the TH —exemplifying that crystals grown *via* seeding may not necessarily have the same crystal form as the seed.

3.2 NPLIN with no polymer additive

All samples without polymer additive exposed to a laser pulse with an energy density of 55–359 mJ cm^{-2}, and some at a lower pulse energy of 27.6 mJ cm^{-2}, crystallized as shown in Fig. 3 (see also ESI,† Table S2). After a single laser pulse, crystals immediately formed along the beam pathway. Initially, thin plate-shaped crystals formed (see Fig. S3† for a close-up image); these grew slowly in size until the emergence of one or more clumps of needle-shaped crystals with a fluffy, cloud-like appearance. The clumps grew more quickly than the plate-shaped crystals and filled the entire vial in approximately 6–10 minutes. In similar experiments previously, Liu *et al.* identified the plate-shaped crystals as AH sodium acetate using single-crystal X-ray diffraction, although the polymorph was not identified.[28,32] Currently 5 crystal structures (forms I to IV and form β) have been determined through X-ray diffraction, with some metastable forms yet to be fully characterized.[33–35] Notably, the known polymorphs are structurally similar, increasing the chances of nucleating multiple polymorphs, and the likelihood of transformations between them. We find that the unit-cell structure of Liu

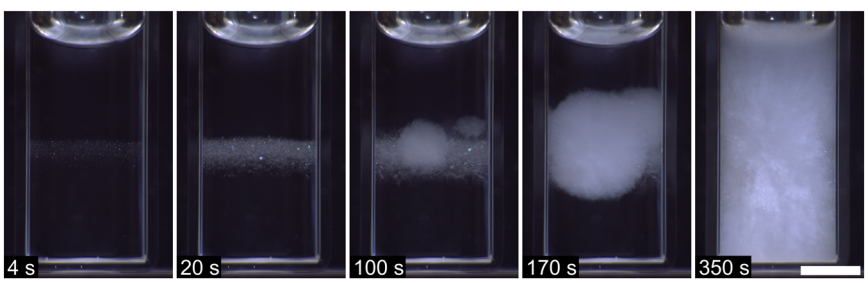

Fig. 3 Growth of sodium acetate crystals from a supersaturated aqueous solution following NPLIN. The incident laser pulse had an energy density of 359 mJ cm^{-2}. From left to right, images show the sample 4, 20, 100, 170 and 350 s after the laser pulse. After the laser pulse, thin, plate-like crystals immediately began growing along the length of the beam path. After 100 s, two clumps of cloud-like needles had emerged; these grew more rapidly than the plate-like crystals and filled the vial after 350 s (5 min 50 s). The scale bar represents 5 mm.

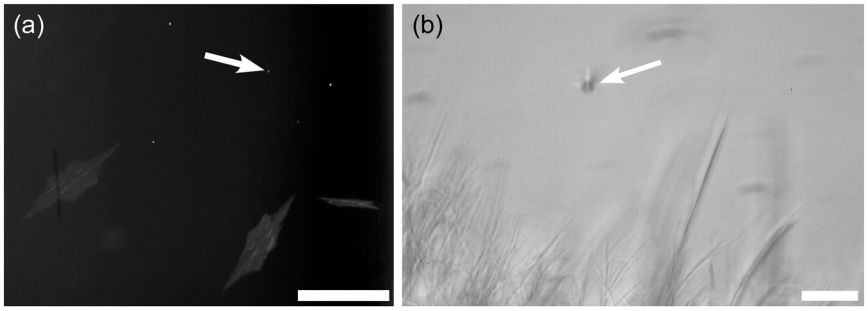

Fig. 4 Sodium acetate crystals growing alongside bubbles in supersaturated aqueous solutions following NPLIN. The incident laser pulse had an energy density of 27.6 mJ cm^{-2}. Both (a) plate-like and (b) needle-like crystals are seen growing alongside bubbles: one bubble in each image is indicated by an arrow, although (a) shows at least 5 bubbles. The bubble in (b) is about 20 μm in diameter. The scale bars represent (a) 1 mm, (b) 100 μm.

et al. matches the orthorhombic form IV, characterized by Dittrich *et al.*[35]

The plate-like crystals always appeared first, with the needle-like clouds emerging later from within the initial band; either the needle-like crystals nucleate more slowly, or they are a result of secondary nucleation. The growth rates of both the plates and needles were substantially slower than TH (350 s *versus* 2.9 s) indicating that presence of the AH–liquid interface is not sufficient to seed nucleation of TH. It seems likely, therefore, that the external seeding experiments (Fig. 2, sec. 3.1) introduced small amounts of TH, perhaps as fine particulates due to handling of the solid in the laboratory,[36,37] or formed at the surface of seed AH crystals due to ambient humidity. These results highlight the utility of techniques such as NPLIN to nucleate metastable crystal forms in sealed environments.

The AH crystal needles may have the same crystal structure as the plates (with the difference in habit due to the change in growth of different crystal faces), or they may be a different polymorph. Hsu *et al.* noted that the habit of form I was needle-like.[33] *In situ* analysis of the two crystal morphologies would be required to determine the polymorph. Although it was possible to pick out plates for X-ray analysis, attempts to retrieve the needles failed due their fragility and the rapid nucleation of TH during handling of the unsealed sample.

The preference for AH crystals by NPLIN in the present system is consistent with previous work on NaBr, where the anhydrous salt was favoured by NPLIN (>90%) but the dihydrate was favoured using other nucleation methods, such as mechanical shock.[16] Barber *et al.* proposed that NPLIN causes a hot cavitation event *via* the particle-heating mechanism, resulting in a preference for dehydrated crystal forms.

In the majority of samples containing no Na-PMAA exposed to low pulse energies of 27.6 mJ cm^{-2} (7/10 samples), small bubbles were observed growing alongside the crystals. These bubbles gradually floated upwards in the solution: see Fig. 4. The formation of stable bubbles and crystals together has not been observed previously using NPLIN. The bubbles survived for at least 10 minutes in the solution (the time when recording was stopped). Water-vapor cavities formed by thermocavitation would be expected to collapse rapidly. Therefore, we attribute these long-lived bubbles to thermochemical reactions that produce gas products, or to nucleation of gas (air) that was dissolved in the solution during preparation: we shall discuss this further in sec. 3.3.

3.3 NPLIN: low and high Na-PMAA additive

Nucleation of crystals only. Solutions containing polymer additive showed three different behaviours on exposure to the laser pulse, depending on the Na-PMAA concentration (see ESI,† Table S3). Nucleation of crystals, with no visible bubbles, was seen in low Na-PMAA samples (4/10 samples). The crystal morphology initially appeared similar to that in the solutions without Na-PMAA; however, the fast-growing,

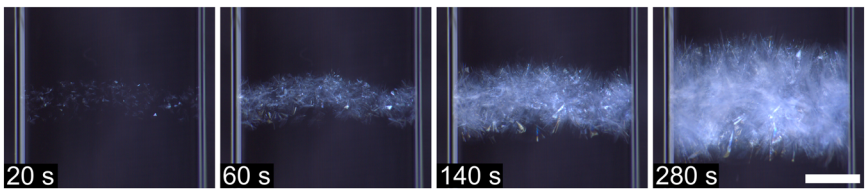

Fig. 5 NPLIN of sodium acetate crystals from a supersaturated aqueous solution containing low Na-PMAA (0.25% w/w). The incident laser pulse had an energy density of 82.9 mJ cm^{-2}. Plate-like crystals grew along the length of the beam path with a morphology identical to those observed in solutions with no Na-PMAA (see Fig. 3). However, the cloud-like clumps of needles did not emerge. Instead, the plate-like crystals continued growing until they filled the vial, which took approximately 15 minutes. The scale bar represents 3 mm.

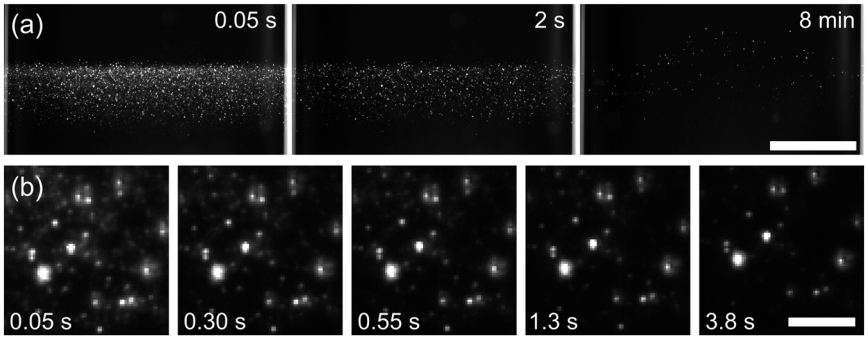

Fig. 6 Bubble formation and dispersal in a supersaturated aqueous solution of sodium acetate containing high Na-PMAA (0.73% w/w), following exposure to a single laser pulse. The incident pulse had an energy density of 166 mJ cm^{-2}. The time after the laser pulse is given in each frame. (a) Only bubbles are apparent, and no crystallization was observed. The bubbles form immediately after the laser pulse along the beam path. After 2 s, the bubbles have not moved significantly, but the intensity of the band of light through the solution has faded. (b) Higher magnification images show that there are smaller bubbles which gradually disappear. Brightness and contrast in all images have been adjusted for clarity. The scale bars represent (a) 3 mm, (b) 0.15 mm.

cloud-like needles did not emerge. Instead, the growth of the crystals continued more slowly with a homogeneous plate-like morphology, taking approximately 15 minutes to fill the entire vial. In Fig. 5 we see that the crystals in the centre of the vial have moved upwards slightly, probably resulting from slow convection in the fluid.

The morphology described here is identical to that observed by Liu *et al.*, but different to that observed by Oliver *et al.* in sodium acetate solutions (C = 17 mol kg^{-1}) containing 0.5% w/w Na-PMAA polymer additive.[27,28] After leaving the supersaturated solution to stand at 20 °C for two weeks, Oliver *et al.* found that AH crystals nucleated spontaneously as very fine needles. The polymer was considered to modify the crystal habit, compared to the much larger plate-like crystals that they observed in solutions without polymer. Their findings appear to be the opposite to the inhibition of the needle-like crystals observed in this work.

Nucleation of bubbles only. The nucleation of bubbles, without any visible crystals, was observed (Fig. 6) in the majority of samples containing high Na-PMAA (98/107 samples) and was sometimes seen in those with low Na-PMAA (3/10 samples). This is consistent with the known inhibitory effect of Na-PMAA on AH nucleation.[26,27] The bubbles appeared along the beam pathway immediately after the laser pulse, along with a band of scattered light, which faded within 0.5 s. On close inspection, the cause of the band was seen to be much smaller bubbles that gradually disappeared, as shown in Fig. 6(b). After some time, the larger bubbles floated upwards slowly, reaching the meniscus (*ca.* 10 mm above the beam) approximately 40 minutes after the laser pulse. There was a distribution in bubble sizes: at a laser pulse energy of 221 mJ cm^{-2}, bubbles with diameters of 10–30 μm were observed (ESI,† Fig. S4).

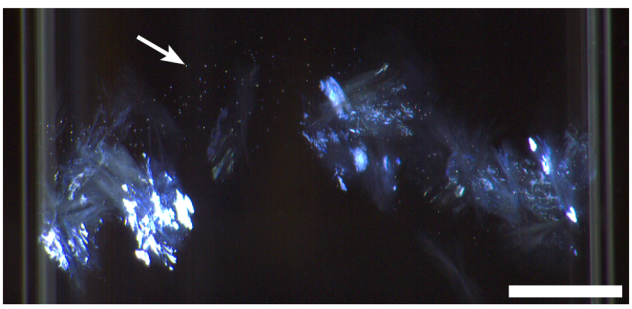

Fig. 7 Sodium acetate crystals growing alongside bubbles in supersaturated aqueous solutions containing low Na-PMAA (0.25% w/w), following NPLIN. The incident laser pulse had an energy density of 82.9 mJ cm^{-2}. The image was taken 7.8 s after the laser pulse. Plate-like crystals grow along the length of the beam path, leaving gaps where small bubbles are clearly visible (an example bubble is indicated by an arrow). Brightness and contrast have been optimized for clarity. The scale bar represents 2 mm.

The stable bubbles observed were too small and few to be able to measure their gas content. As proposed above, these bubbles can be attributed to gas produced by thermochemistry, or gas that was previously dissolved in the solution. In the nanoparticle-heating mechanism for NPLIN, the particles are expected to reach temperatures $T > 5000$ K, significantly higher than the critical temperature (*e.g.*, for water, T_c = 647 K).[10] Such high temperatures are sufficient for thermochemical splitting of water to produce, *e.g.*, H_2, O_2, and products of reactions involving solute, *e.g.*, CO. The bubbles might also contain one or more components of air (N_2, O_2, Ar, CO_2) that was dissolved in the liquid during sample preparation and handling. These gases show retrograde solubility in water, meaning that the solubility decreases with increasing temperature. Therefore, the resulting high temperatures would create a region around the particle that was supersaturated with gas.[10,38] Transient thermocavities might act as seeds for the nucleation of gas bubbles. Ward *et al.* proposed a mechanism whereby an influx of dissolved gas results in the spontaneous growth of bubbles, providing the cavity reaches a critical size, for a solution that was supersaturated with CO_2 gas.

The smaller objects that fade away (Fig. 6) are likely to be small bubbles of gas which redissolve rather than grow. If

Table 1 Percentage of sodium acetate samples at different Na-PMAA concentrations showing NPLIN of crystals, nucleation of crystals together with bubbles, or nucleation of bubbles. The incident laser pulse had an energy density of 82.9 mJ cm^{-2} for all samples. Percentages do not add up to 100% in the last row, due to samples that did not react to the laser

Na-PMAA concentration/(% w/w)	Number of samples tested	Percentage of samples		
		Crystals	Crystals and bubbles	Bubbles
0 (zero)	13	100	0	0
0.25 (low)	10	40	30	30
0.73 (high)	31	0	13	84

the fading smaller objects were instead due to incandescence of particles or transient cavitation, they would be expected to fade within 0.05 s (a single frame after the initiating laser pulse), whereas the objects observed lasted for at least 0.5 s. Incandescence results from blackbody emission due to high temperatures (>2000 K) achieved by the laser heating. In an aqueous liquid, the duration of emission has been observed to be similar to the duration of the laser pulse (5 ns in the present case).[39] The lifetime of laser-induced cavitation bubbles have been measured to have lifetimes on the order of 100 μs.[6,40] Small bubbles will dissolve due to the higher internal pressure according to the Laplace relationship,[41]

$$\Delta p = p_{\text{int}} - p_{\text{ext}} = \frac{2\gamma}{r} \quad (1)$$

where p_{int} is the internal pressure, p_{ext} is the external pressure (atmospheric pressure in this case), γ is the gas–liquid interfacial tension, and r is the radius of the bubble. After careful review of images, objects which faded away quickly after the laser pulse were also seen during crystal formation in solutions without Na-PMAA, but were less obvious. The polymer Na-PMAA would be expected to act as a surfactant to stabilize the bubbles, *i.e.*, by reducing the interfacial tension in eqn (1), so that bubbles with the same radius require a lower internal pressure to survive. Along with the ability of Na-PMAA to inhibit nucleation of AH crystals, this stabilization would explain why the most bubbles were observed in solutions with high Na-PMAA.

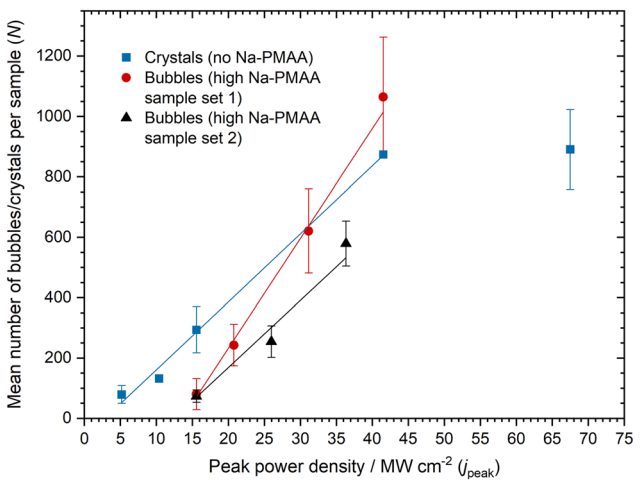

Fig. 8 The mean number of crystals or bubbles counted in NPLIN of supersaturated aqueous sodium acetate samples *versus* the peak power density of the laser pulse. Samples containing no Na-PMAA produced crystals on exposure to the laser (solid squares); whereas samples containing high Na-PMAA (0.73% w/w) produced bubbles. Two high Na-PMAA sample sets were used; the experimental data for these are represented by red circles and black triangles. The solid lines represent linear fits of the data (the point at 70 MW cm^{-2} was excluded). Error bars represent the standard errors of the means.

Nucleation of bubbles and crystals. In sec. 3.2 we showed that both crystals and bubbles were observed in a few cases in samples containing no Na-PMAA. Both bubbles and crystals were also observed in some samples containing low Na-PMAA (3/10 samples) or containing high Na-PMAA (8/107 samples) at low laser pulse energies. In general, bubbles appeared immediately following the laser pulse and began to gradually move upwards. After a few seconds, a small number of crystals became distinguishable within the band of bubbles. The crystals had a plate-like morphology; the emergence of the cloud-like needles did not occur. Since crystals at their early stage of growth were indistinguishable from bubbles, these observations were most clear when crystals did not form along the entire beam path. An example image where both crystals and bubbles can clearly be seen is shown in Fig. 7. In a few cases, crystal growth was seen to be associated with a specific bubble; however, the similarity of crystals and bubbles at early times meant this could not be confirmed unambiguously.

The formation of crystals and stable bubbles is an intermediate behaviour, as the nucleation transitions from predominantly crystal nucleation to predominantly bubble nucleation with the increase of the polymer additive. This transition can be seen clearly in Table 1, which compares samples with different Na-PMAA concentrations exposed to laser pulses with the same energy density.

3.4 Laser pulse-energy dependence

The dependence of the crystal count and bubble count on laser energy was investigated in samples containing no Na-PMAA and high Na-PMAA, respectively. Crystals and bubbles were counted using image analysis software, ImageJ (see ESI† for details).[42] We report the results in terms of the peak power density of the laser pulse, to facilitate comparison with previous NPLIN studies. For all data sets, the number of bubbles or crystals showed a linear dependence at low peak power densities: see Fig. 8. The data point at 70 MW cm^{-2} suggests that a plateau is reached at higher power densities,

Table 2 Threshold power densities and labilities obtained for the formation of bubbles in two sample sets with polymer additive (high Na-PMAA), and the formation of crystals in a single sample set with no polymer additive. Results were obtained using a linear fit in the form of eqn (2) with the exponent *a* fixed at 1. Uncertainties are standard errors returned from the least-squares fitting procedures

Sample set	Threshold peak power density (j_0)/MW cm^{-2}	Lability (m)/cm^2 MW^{-1}
High Na-PMAA set 1 (bubbles)	13.6 ± 1.2	36.4 ± 1.8
High Na-PMAA set 2 (bubbles)	12.4 ± 3.6	22.2 ± 3.5
No Na-PMAA (crystals)	2.9 ± 1.2	22.5 ± 1.2

which is consistent with trends in previous studies of NPLIN.[43,44]

Ward *et al.*[10] previously studied LIN of CO_2 bubbles from supersaturated carbonated aqueous sucrose solutions using laser parameters (power, duration, wavelength) similar to the present work. The bubble counts observed were modelled using the following function:

$$N = m(j_{peak} - j_0)^a, \quad (j_{peak} \geq j_0)$$

$$N = 0, \quad (j_{peak} < j_0) \tag{2}$$

where N is the number of bubbles, j_{peak} is the peak power density, j_0 is the threshold power density (below which nucleation does not occur) and m is the lability (a measure of the susceptibility of the sample to LIN). They found that the exponent a, was very close to 2 (*i.e.*, a quadratic dependence). For the present system, non-linear least-squares fitting of the bubble counts for high Na-PMAA samples (set 1) gave a = 1.25 ± 0.03; similar fitting of the crystal counts in no Na-PMAA samples (excluding the point at 70 MW cm^{-2}) gave a = 1.1 ± 0.3. There is no significant difference between these values, which suggests that crystals and bubbles produced by NPLIN in this system have a common origin, *i.e.*, cavitation induced by particle heating.

The results of fitting the data with a linear model (fixing a = 1) are given in Table 2 and shown in Fig. 8. The fitted parameters obtained are comparable to previous work, *e.g.*, on NPLIN of KCl solutions in aqueous agarose gels (j_0 = 8.3 ± 2.2 MW cm^{-2} and m = 6.6 ± 0.5 cm^2 MW^{-1}; S = 1.06 in 0.5% w/w agarose).[43] The threshold powers and the labilities can be explained by considering a population of impurity nanoparticles with different sizes in the nanoparticle-heating mechanism. At low laser pulse energies, particles will not reach a sufficient temperature to produce a cavity. As the pulse energy is increased, first the larger particles and then smaller particles will produce cavities that result in crystals or bubbles. At the highest energies, all particles are activated, and there is no increase in N, *i.e.*, the count reaches a plateau. The smaller gas bubbles that redissolve are likely to be those formed by heating of smaller particles. The values for the threshold power densities (j_0) are higher for bubble nucleation than crystal nucleation. This may be due to the increased viscosity of solutions containing high Na-PMAA, meaning that particles require more energy for the cavity to expand to a critical size to yield stable bubbles.

Finally, we consider the question of whether stable gas bubbles are directly involved in the mechanism for NPLIN of crystals. It is possible that a stable bubble provides an interface for heterogeneous nucleation of the solid. This suggestion was first made by Knott *et al.*, who showed that, when gently shaken, aqueous solutions supersaturated with both glycine and argon nucleated first gas bubbles followed by many glycine crystals.[45] Control experiments with saturated argon but supersaturated glycine produced no crystals; experiments with no argon produced only a few crystals. As a counterpoint, Briard *et al.* studied NPLIN of aqueous supersaturated solutions of potassium sulfate (K_2SO_4).[46] Solutions that had been degassed by sonication were compared against solutions saturated with air, N_2, or CO_2. No significant differences were observed in the time for nucleation of the first crystals (induction time) or the probability of crystal nucleation, suggesting that dissolved gas is not involved in the NPLIN mechanism. It may be, however, that thermochemical gas production is an important step in NPLIN of solids.

4. Conclusions

In summary, we have conducted an in-depth study of the nucleation of supersaturated sodium acetate solutions, including the effects of Na-PMAA polymer additive. We found that AH seeds produced TH sodium acetate crystals either with or without polymer additive, exemplifying that the form of crystals grown cannot always be controlled by the seed employed. On the other hand, NPLIN invariably produced AH sodium acetate, demonstrating the utility of LIN methods for nucleating metastable crystal forms. The formation of crystals and stable bubbles was observed in NPLIN of supersaturated aqueous sodium acetate solutions, with the outcome depending on both the laser pulse power and the concentration of additive Na-PMAA. Approximately similar numbers of crystals and bubbles were formed, and counts for both showed a threshold and a linear dependence on pulse energy at lower laser powers. The results suggest that both crystals and bubbles are formed by cavitation events obtained through the particle-heating mechanism for NPLIN. Whether stable bubbles are necessary for NPLIN of crystals in this mechanism is still unresolved, and further experiments to resolve this are ongoing.

Data availability

Data employed in this study are available *via* the Edinburgh DataShare repository (DOI: **https://doi.org/10.7488/ds/7748**).

Conflicts of interest

There are no conflicts to declare.

Acknowledgements

The authors thank Professors Colin Pulham and Philip Camp for useful discussions. We are grateful to the Engineering and Physical Sciences Research Council (EP/N509644/1); CMAC Future Manufacturing Research Hub (**http://www.cmac.ac.uk**) and The Royal Society (IEC\R3\193037) for supporting this work.

References

1 T. Sugiyama and S.-F. Wang, Manipulation of Nucleation and Polymorphism by Laser Irradiation, *J. Photochem. Photobiol., C*, 2022, **52**, 100530, DOI: **10.1016/j.jphotochemrev.2022.100530**.

2 C.-S. Wu, P.-Y. Hsieh, K. Yuyama, H. Masuhara and T. Sugiyama, Pseudopolymorph Control of l-Phenylalanine Achieved by Laser Trapping, *Cryst. Growth Des.*, 2018, **18**(9), 5417–5425, DOI: **10.1021/acs.cgd.8b00796**.

3 B. A. Garetz, J. E. Aber, N. L. Goddard, R. G. Young and A. S. Myerson, Nonphotochemical, Polarization-Dependent, Laser-Induced Nucleation in Supersaturated Aqueous Urea Solutions, *Phys. Rev. Lett.*, 1996, **77**(16), 3475–3476, DOI: **10.1103/PhysRevLett.77.3475**.

4 W. Li, A. Ikni, P. Scouflaire, X. Shi, N. El Hassan, P. Gémeiner, J.-M. Gillet and A. Spasojević-de Biré, Non-Photochemical Laser-Induced Nucleation of Sulfathiazole in a Water/Ethanol Mixture, *Cryst. Growth Des.*, 2016, **16**(5), 2514–2526, DOI: **10.1021/acs.cgd.5b01526**.

5 K. Nakamura, Y. Hosokawa and H. Masuhara, Anthracene Crystallization Induced by Single-Shot Femtosecond Laser Irradiation: Experimental Evidence for the Important Role of Bubbles, *Cryst. Growth Des.*, 2007, **7**(5), 885–889, DOI: **10.1021/cg060631q**.

6 A. Soare, R. Dijkink, M. R. Pascual, C. Sun, P. W. Cains, D. Lohse, A. I. Stankiewicz and H. J. M. Kramer, Crystal Nucleation by Laser-Induced Cavitation, *Cryst. Growth Des.*, 2011, **11**(6), 2311–2316, DOI: **10.1021/cg2000014**.

7 H. Y. Yoshikawa, R. Murai, H. Adachi, S. Sugiyama, M. Maruyama, Y. Takahashi, K. Takano, H. Matsumura, T. Inoue, S. Murakami, H. Masuhara and Y. Mori, Laser Ablation for Protein Crystal Nucleation and Seeding, *Chem. Soc. Rev.*, 2014, **43**(7), 2147–2158, DOI: **10.1039/c3cs60226e**.

8 E. R. Barber, N. L. H. Kinney and A. J. Alexander, Pulsed Laser-Induced Nucleation of Sodium Chlorate at High Energy Densities, *Cryst. Growth Des.*, 2019, **19**(12), 7106–7111, DOI: **10.1021/acs.cgd.9b00951**.

9 A. J. Alexander and P. J. Camp, Non-Photochemical Laser-Induced Nucleation, *J. Chem. Phys.*, 2019, **150**(4), 040901, DOI: **10.1063/1.5079328**.

10 M. R. Ward, W. J. Jamieson, C. A. Leckey and A. J. Alexander, Laser-Induced Nucleation of Carbon Dioxide Bubbles, *J. Chem. Phys.*, 2015, **142**(14), 144501, DOI: **10.1063/1.4917022**.

11 C. T. Avedisian, The Homogeneous Nucleation Limits of Liquids, *J. Phys. Chem. Ref. Data*, 1985, **14**(3), 695–729, DOI: **10.1063/1.555734**.

12 N. Javid, T. Kendall, I. S. Burns and J. Sefcik, Filtration Suppresses Laser-Induced Nucleation of Glycine in Aqueous Solutions, *Cryst. Growth Des.*, 2016, **16**(8), 4196–4202, DOI: **10.1021/acs.cgd.6b00046**.

13 M. R. Ward, A. M. Mackenzie and A. J. Alexander, Role of Impurity Nanoparticles in Laser-Induced Nucleation of Ammonium Chloride, *Cryst. Growth Des.*, 2016, **16**(12), 6790–6796, DOI: **10.1021/acs.cgd.6b00882**.

14 M. Briard, C. Brandel and V. Dupray, Strong Enhancement of Nucleation Efficiency of Aqueous Ethylenediamine Sulfate Solutions by Nonphotochemical Laser-Induced Nucleation: Investigations on the Role of Solid Impurities in the Mechanism, *Cryst. Growth Des.*, 2023, **23**(10), 7169–7178, DOI: **10.1021/acs.cgd.3c00588**.

15 Y. Liu, M. H. van den Berg and A. J. Alexander, Supersaturation Dependence of Glycine Polymorphism Using Laser-Induced Nucleation, Sonocrystallization and Nucleation by Mechanical Shock, *Phys. Chem. Chem. Phys.*, 2017, **19**(29), 19386–19392, DOI: **10.1039/C7CP03146G**.

16 E. R. Barber, M. R. Ward, A. D. Ward and A. J. Alexander, Laser-Induced Nucleation Promotes Crystal Growth of Anhydrous Sodium Bromide, *CrystEngComm*, 2021, **23**(47), 8451–8461, DOI: **10.1039/D1CE01180D**.

17 M. Kenisarin and K. Mahkamov, Salt Hydrates as Latent Heat Storage Materials:Thermophysical Properties and Costs, *Sol. Energy Mater. Sol. Cells*, 2016, **145**, 255–286, DOI: **10.1016/j.solmat.2015.10.029**.

18 S. Ben Romdhane, A. Amamou, R. Ben Khalifa, N. M. Saïd, Z. Younsi and A. Jemni, A Review on Thermal Energy Storage Using Phase Change Materials in Passive Building Applications, *J. Build. Eng.*, 2020, **32**, 101563, DOI: **10.1016/j.jobe.2020.101563**.

19 B. Sandnes, The Physics and the Chemistry of the Heat Pad, *Am. J. Phys.*, 2008, **76**(6), 546–550, DOI: **10.1119/1.2830533**.

20 W. F. Green, The "Melting-Point" of Hydrated Sodium Acetate: Solubility Curves, *J. Phys. Chem.*, 1908, **12**(9), 655–660, DOI: **10.1021/j150099a002**.

21 J. Schröder and K. Gawron, Latent Heat Storage, *Int. J. Energy Res.*, 1981, **5**(2), 103–109, DOI: **10.1002/er.4440050202**.

22 J. Guion, J. D. Sauzade and M. Laügt, Critical Examination and Experimental Determination of Melting Enthalpies and Entropies of Salt Hydrates, *Thermochim. Acta*, 1983, **67**(2), 167–179, DOI: **10.1016/0040-6031(83)80096-3**.

23 K. K. Meisingset and F. Grønvold, Thermodynamic Properties and Phase Transitions of Salt Hydrates between 270 and 400 K III. CH3CO2Na·3H2O, CH3CO2Li·2H2O, and

(CH3CO2)2Mg·4H2O, *J. Chem. Thermodyn.*, 1984, **16**(6), 523–536, DOI: **10.1016/0021-9614(84)90003-X**.

24 T. Wada, R. Yamamoto and Y. Matsuo, Heat Storage Capacity of Sodium Acetate Trihydrate during Thermal Cycling, *Sol. Energy*, 1984, **33**(3), 373–375, DOI: **10.1016/0038-092X(84)90169-5**.

25 Z. Yinping, J. Yi and J. Yi, A Simple Method, the T-History Method, of Determining the Heat of Fusion, Specific Heat and Thermal Conductivity of Phase-Change Materials, *Meas. Sci. Technol.*, 1999, **10**(3), 201, DOI: **10.1088/0957-0233/10/3/015**.

26 D. E. Oliver, A. J. Bissell, X. Liu, C. C. Tang and C. R. Pulham, Crystallisation Studies of Sodium Acetate Trihydrate – Suppression of Incongruent Melting and Sub-Cooling to Produce a Reliable, High-Performance Phase-Change Material, *CrystEngComm*, 2021, **23**(3), 700–706, DOI: **10.1039/D0CE01454K**.

27 D. E. Oliver, *PhD thesis*, University of Edinburgh, 2014.

28 Y. Liu, *PhD thesis*, University of Edinburgh, 2017.

29 B. Lindinger, R. Mettin, R. Chow and W. Lauterborn, Ice Crystallization Induced by Optical Breakdown, *Phys. Rev. Lett.*, 2007, **99**(4), 045701.

30 N. Iefuji, R. Murai, M. Maruyama, Y. Takahashi, S. Sugiyama, H. Adachi, H. Matsumura, S. Murakami, T. Inoue, Y. Mori, Y. Koga, K. Takano and S. Kanaya, Laser-Induced Nucleation in Protein Crystallization: Local Increase in Protein Concentration Induced by Femtosecond Laser Irradiation, *J. Cryst. Growth*, 2011, **318**(1), 741–744, DOI: **10.1016/j.jcrysgro.2010.10.068**.

31 E. R. Barber, *PhD thesis*, University of Edinburgh, 2022.

32 Y. Liu, H. He and Y. Liu, Morphology Control of Laser-Induced Dandelion-like Crystals of Sodium Acetate through the Addition of Acidic Polymers, *J. Appl. Crystallogr.*, 2021, **54**(4), 1111–1120.

33 L.-Y. Hsu and C. E. Nordman, Structures of Two Forms of Sodium Acetate, Na+.C2H3O2-, *Acta Crystallogr., Sect. C: Cryst. Struct. Commun.*, 1983, **39**(6), 690–694.

34 R. Helmholdt, Ab Initio Crystal Structure Determination of β-Sodium Acetate from Powder Data, *Z. Kristallogr.*, 1998, **213**(11), 596–598, DOI: **10.1524/zkri.1998.213.11.596**.

35 B. Dittrich, J. Bergmann, P. Roloff and G. J. Reiss, New Polymorphs of the Phase-Change Material Sodium Acetate, *Crystals*, 2018, **8**(5), 213, DOI: **10.3390/cryst8050213**.

36 J. D. Dunitz and J. Bernstein, Disappearing Polymorphs, *Acc. Chem. Res.*, 1995, **28**(4), 193–200, DOI: **10.1021/ar00052a005**.

37 D.-K. Bučar, R. W. Lancaster and J. Bernstein, Disappearing Polymorphs Revisited, *Angew. Chem., Int. Ed.*, 2015, **54**(24), 6972–6993, DOI: **10.1002/anie.201410356**.

38 J. O. Sindt, A. J. Alexander and P. J. Camp, Effects of Nanoparticle Heating on the Structure of a Concentrated Aqueous Salt Solution, *J. Chem. Phys.*, 2017, **147**(21), 214506, DOI: **10.1063/1.5002002**.

39 S. Zelensky, Laser-Induced Heat Radiation of Suspended Particles: A Method for Temperature Estimation, *J. Opt. A: Pure Appl. Opt.*, 1999, **1**(4), 454, DOI: **10.1088/1464-4258/1/4/306**.

40 P. A. Quinto-Su, K. Y. Lim and C.-D. Ohl, Cavitation Bubble Dynamics in Microfluidic Gaps of Variable Height, *Phys. Rev. E: Stat., Nonlinear, Soft Matter Phys.*, 2009, **80**(4), 047301, DOI: **10.1103/PhysRevE.80.047301**.

41 S. F. Jones, G. M. Evans and K. P. Galvin, Bubble Nucleation from Gas Cavities — a Review, *Adv. Colloid Interface Sci.*, 1999, **80**(1), 27–50, DOI: **10.1016/S0001-8686(98)00074-8**.

42 J. Schindelin, I. Arganda-Carreras, E. Frise, V. Kaynig, M. Longair, T. Pietzsch, S. Preibisch, C. Rueden, S. Saalfeld, B. Schmid, J.-Y. Tinevez, D. J. White, V. Hartenstein, K. Eliceiri, P. Tomancak and A. Cardona, Fiji: An Open-Source Platform for Biological-Image Analysis, *Nat. Methods*, 2012, **9**(7), 676–682, DOI: **10.1038/nmeth.2019**.

43 C. Duffus, P. J. Camp and A. J. Alexander, Spatial Control of Crystal Nucleation in Agarose Gel, *J. Am. Chem. Soc.*, 2009, **131**(33), 11676–11677, DOI: **10.1021/ja905232m**.

44 T. Hua, O. Gowayed, D. Grey-Stewart, B. A. Garetz and R. L. Hartman, Microfluidic Laser-Induced Nucleation of Supersaturated Aqueous KCl Solutions, *Cryst. Growth Des.*, 2019, **19**(6), 3491–3497, DOI: **10.1021/acs.cgd.9b00362**.

45 B. C. Knott, J. L. LaRue, A. M. Wodtke, M. F. Doherty and B. Peters, Communication: Bubbles, crystals, and laser-induced nucleation, *J. Chem. Phys.*, 2011, **134**, 171102, DOI: **10.1063/1.3582897**.

46 M. Briard, C. Brandel, S. Morin-Grognet, G. Coquerel and V. Dupray, Potassium Sulfate: A New Candidate to Explore Non-Photochemical Laser-Induced Nucleation Mechanisms, *Crystals*, 2021, **11**(12), 1571, DOI: **10.3390/cryst11121571**.

